16

STEWARD-1560

PREPRINTS

of the

STEWARD OBSERVATORY

THE UNIVERSITY OF ARIZONA
TUCSON, ARIZONA 85721-0065 U.S.A.

No. 1560

Fermilab Library
0 1160 0071832 4

LUMINOSITY FUNCTION OF GALAXIES IN THE NEARBY UNIVERSE: THE LOW-LUMINOSITY END OF THE NUCLEAR ACTIVITY SEQUENCE

BALTASAR VILA-VILARO*

Nobeyama Radio Observatory†, Minamimaki-mura, Minamisaku-gun, Nagano 384-1305
E-mail (BVV): bvila@as.arizona.edu

Note J

TO APPEAR IN PUBLICATIONS OF THE ASTRONOMICAL SOCIETY OF JAPAN

*Present address: Steward Observatory, The University of Arizona, 933 N. Cherry Avenue, Tucson, Arizona 85721, U.S.A.

†Nobeyama Radio Observatory (NRO) is a branch of the National Astronomical Observatory, an inter-university research institute operated by the Ministry of Education, Science, Sports andCulture.

Luminosity Function of Galaxies in the Nearby Universe: The Low-Luminosity End of the Nuclear Activity Sequence

Baltasar VILA-VILARO*
Nobeyama Radio Observatory[†] *Minamimaki-mura, Minamisaku-gun, Nagano 384-1305*
E-mail(BVV): bvila@as.arizona.edu

(Received ; accepted)

Abstract

We present an estimate of the shape of the luminosity functions in the nearby Universe for the 4 types of extragalactic nuclear activity cited in Ho et al. (1997), i.e., HII, LINER, Transition and Seyfert galaxies, based on a magnitude limited complete sample of objects selected from the same work. This sample reaches includes quite weaker nuclear emission objects than previous works, which allows to assess the low-luminosity ends of the nuclear activity sequance for each of the types. It is found that three of the classes (LINER, Transition and Seyferts) have very similar luminosity function shapes and basically seem to differ only in the relative numbers. HII objects tend to be found in different hosts (lower luminosity galaxies) and seem to have a bimodal luminosity function, with a fairly large proportion of Im and dwarf galaxies in this class that are superposed to a more Schechter-like luminosity function. Several observational properties also suggest that Transition objects are actually LINERs contaminated by HII regions, and should be included in that category. Our fits further suggest the presence of a substantial number of low luminosity host Seyferts in the nearby Universe. The distribution of absolute magnitudes for Seyferts type 1 and 2 is very similar in our sample. The possibility that the LINER class encompasses several different classes of objects is also discussed.

Key words: Galaxies: active — Galaxies: evolution — Galaxies: nuclei — Galaxies: general — Luminosity function

1. Introduction

Broadly speaking, two main types of activity have been found in the nuclear regions of galaxies, star formation and that of Active Galactic Nuclei (hereafter AGN). Although a consensus has still not been reached on the nature of the latter, models that involve accretion onto a very massive black hole lying at the center of the host galaxy seem to be the most widely accepted (Rees 1984). Numerous spectroscopic and photometric studies reveal that both phenomena seem to cover a wide range of luminosities (line emission and continnum that can be associated directly to each mechanism) and show strong cosmological evolution. Furthermore, some objects seem to show both kinds of activity at the same time, which has led some authors to suggest that there may exist an evolutionary connection between them (Heckman et al. 1997).

The classification of star-forming objects has been mainly based on the inferred rate of star formation necessary to explain either their optical/NIR line emission fluxes or their FIR continuum (in the case of the Ultraluminous IR Galaxies). The highest rates of star formation are associated with Starburst Galaxies, which seem to be producing stars at rates of hundreds of times those in the disks of normal spirals. They are often found in strongly interacting systems (most of them are isolated, though)(Moorwood 1996). The lower end of the star formation sequence is occupied by the "HII region" galaxies with emission line luminosities that can be thousands of times smaller than nuclear starbursts (Ho et al. 1997). The density of starburst galaxies seems to increase with redshift, possibly as a result of the larger number of interacting objects in the earlier Universe (Moorwood 1996).

Currently the AGN family contains many classes of objects, but their most widely used broad classification is based on the intrinsic radio continuum power of the hosts (Kim and Elvis 1999). "Radio quiet" AGN (weak radio emmitters) are the most abundant, and their subclassification has been based on intrinsic nuclear bolometric luminosities (arbitrary limit). Both quasars (high luminosity) and Seyfert galaxies (intermedate luminosity) seem to be produced by the same kind of mechanism

* Present address: Steward Observatory, The University of Arizona, 933 N. Cherry, Tucson, Arizona 85721, U.S.A..

† Nobeyama Radio Observatory (NRO) is a branch of the National Astronomical Observatory, an inter-university research institute operated by the Ministry of Education, Science, Sports and Culture.

and the difference between these classes is merely the luminosity radiated by the central energy source (Bregman 1990). The low luminosity end of the radio quiet objects seems to be occupied by the LINERs, but still no agreement has been reached on whether they are true AGN or not. Alternative explanations include shock excitation and star formation (c.f., Filippenko 1996). Since intermediate to low luminosity AGNs are difficult to detect at high redshifts, at present strong cosmological evolution has only been reported for quasars (c.f., Choi et al. 1999).

Several attempts have been made to derive the luminosity functions of both kinds of nuclear activity for different subclasses of objects (Koehler et al. 1997, Kim et al. 1998 and references therein). However, most of these have been based on optical flux-limited samples that cover wide ranges in distance. Therefore, due to the combined effect of Malmquist bias in the sampling of the host galaxies (weak galaxies are not included at large redshifts) and the lack of deep nuclear line emission surveys in the nearby Universe, these have not been able to address the faint end of the luminosity functions in each case (activity in intrinsically weak/small galaxies) or the relative number of each of the subclasses (only the bright nuclear emission objects were included). In order to overcome these previous problems, Ho et al. (1997) undertook a systematic deep spectroscopic survey of the northern galaxies in the RSA catalogue (Sandage and Tammann 1981). Using the results of their survey, we present in this paper estimates of the luminosity functions of different kinds of active objects in the nearby Universe that include weak nuclear emission galaxies. These estimates are compared with those reported previously for brighter objects. Implications for the evolutionary scenarios between starburst and AGNs are inferred, and the possible connection between the different types of AGNs is discussed.

We present the sample that will be used in this paper in Section 2. Since the definition of the sample is a very important matter in any derivation of luminosity functions, we have made a fairly detailed description of its selection and contents. Section 3 presents the methods that we used to determine the luminosity functions and the results of our fits are presented in Section 4. Section 5 presents a discusion of the main issues raised by this paper.

2. The Sample

As mentioned above, the objective of this paper is to derive the luminosity functions of different kinds of active objects avoiding as much as possible the pitfalls of previous work (undersampling of weak galaxies and weak nuclear emission objects). The former problem can be overcome with the use of catalogues with well-known completeness properties that sample the nearby universe (where the weaker objects can still be detected by current telescopes). The latter problem involves a systematic and deep spectroscopic survey of the nuclear regions of all the galaxies in such catalogues. This will require the use of both large optical telescopes and also good stellar absorption decontamination techniques to detect weak emission lines hidden by the bulge stellar spectrum. The only work which fulfills the above requirements is that of Ho et al. (1997).

Ho et al.'s spectroscopic survey, consists of high-quality, long slit, optical spectra of moderate resolution of the nuclear region (a few100 pcs) of almost every bright galaxy in the northern sky. They were obtained with the Hale 5m telescope at Palomar Observatory. Their sample is based on the Revised Shapley-Ames Catalog of Bright Galaxies (RSA, Sandage and Tammann 1981) and includes all objects with $\delta > 0^o$ and $B_T \leq 12.5$ mag both in the main catalogue and in the "Appendix of Additional Bright Galaxies" (necessary to improve the completeness of the catalog). A few additional objects (15) of special or historical interest that do not adjust to the above criteria were also included in their sample. Their final sample consisted of 503 galaxies of which 486 were observed. A very detailed description of the data reduction procedures used can be found in Ho et al. (1997), but we note that their excellent bulge stellar absorption decontamination technique allows the detection of very weak nuclear line emission and also guarantees that the line ratios that are used for classification of the nuclear activity are consistent. The fact that lower sensitivity spectroscopic surveys of the nearby universe (the region sampled by the RSA catalog) done in the past have failed to detect the presence of many strong nuclear line emitters already suggests that the results of the Ho et al.'s survey will sample the low luminosity end (in nuclear emission) of nuclear activity. This is confirmed by the average line fluxes (the median nuclear Hα flux in this sample is 100 times weaker than archetypical Seyfert galaxies).

Ho et al. use several line ratios that are not much affected by reddening and that have been traditionally used in the so-called diagnostic diagrams to separate the gas ionization mechanisms (Baldwin et al. 1981), and classify the objects in their sample into 5 broad categories (see Table 5 in Ho et al. 1997 for the values used): No Emission Objects, HII nuclei, Seyfert galaxies, LINERs and Transition Objects. As the name itself indicates, No Emission Objects are those that show no nuclear emission lines after careful decontamination of the bulge stellar component. These objects turn out to be a minority (only 14% of the 486 objects), which indicates that weak nuclear emission is almost universal in galaxies. HII nuclei are those that have spectra similar to those of disk HII regions and will be associated to star forming nuclei. The distinction between Seyferts and LINERs is somewhat arbitrary since their line ratios smoothly merge at

intermediate excitation levels ([OIII]/Hβ ratio) in the diagnostic diagrams, but LINERs clearly seem to encompass lower excitation objects than Seyferts. Both Seyferts and LINERs are further subdivided in types 1 and 2 according to the presence or lack of broad Balmer lines in their spectra. Transition objects are a class postulated by Ho and Filippenko (1993), which show intermediate line ratios between those typical of HII regions and those of LINERs. Of the total sample of line-emitting objects, HII seem to be in about half of the objects and the second most abundant class are the LINERs (about a fourth).

Since we intend to derive the luminosity functions in the nearby universe for the 4 categories of nuclear activity included in Ho et al.'s survey, we need to select a subsample that is complete up to a certain magnitude and without any systematic errors in the absolute magnitude estimates. We proceeded in the following way: we first eliminated from the sample all objects (7) that had negative declinations or B_T magnitudes larger than 12.5 mag, since they had been clearly added as special interest to Ho's sample and therefore do not follow their sample selection criteria. The apparent B magnitudes of the objects left that were listed in the *main* RSA catalog (good apparent magnitude estimates) were then compared with those listed in the RC3 catalogue (de Vaucouleurs et al. 1991) to infer any possible systematic offsets. A Kolmogorov-Smirnov test showed that the magnitudes from both catalogues are compatible within the errorbars quoted in the RC3 catalog. Since, as noted by the authors, the B_T estimates for the objects in the *Appendix* of the RSA catalog are quite poor, and due to the good agreement of the magnitudes for the objects in the main RSA catalog and the RC3, we decided to use the values cited in the latter for the objects in Ho's list that are listed in the abovementioned Appendix. Taking into account the considerations of the completeness of the RSA catalog with magnitude (Sandage et al. 1979), we decided to only include in the sample those objects that had $B_T \leq 12.5$ in the RC3 from both the main and Appendix listings, which rendered a final subsample from Ho's original (486) of 448 objects. Of these, 396 have nuclear emission lines according to Ho et al. (1997), and their breakdown in activity categories is listed in Table 1.

Since Ho's sample and our subsample are extracted from the RSA catalog, it should be expected that the completeness properties are the same. The completeness of the RSA *main* catalog is amply discussed in Sandage et al. (1979). The RSA is complete down to B_T=12 mag and the completeness becomes progressively worse at larger magnitudes (at 12.5 mag the catalog is only 80% complete). The same work also shows that this completeness does not depend on galactic latitude (i.e., b). Since the number of objects added to our subsample in the magnitude range 12-12.5 mag from the Appendix of the RSA (48) is consistent with the number of objects needed to make the sample complete to 12.5 mag (deduced from the completeness function in Sandage et al. 1979), we consider that our subsample represents most of the northern hemisphere galaxies with $B_T \leq 12.5$ mag, and therefore, no calculation of the completeness function is done when deriving the luminosity functions below.

Table 1. Percentage breakdown of our subsample.

Type	Number	Relative %*	Total %*
HII	198	50.0	44.2
LINER	88	22.2	19.6
Seyfert	45	11.4	10.0
Transition	65	16.4	14.5

* Relative percentages are evaluated with respect to the number of emission line objects in the subsample (396) while total percentages are relative to the total number of objects in the subsample (448).

Since our subsample overlaps with the "Nearby Galaxy Catalog" by Tully (1988), who derived distances to galaxies using a model that assumes a retardation of the Hubble flow for the Galaxy of 300 km s^{-1} due to the mass of the Virgo cluster, a Hubble constant of 75 km s^{-1} Mpc^{-1} and a distance to the Virgo cluster of 16.8 Mpc, we used the distance values listed there for consistency in deriving the absolute mangitudes. For the few objects not listed in that catalog, the distance was derived from the recession velocity (RC3) using the same value of the Hubble constant as in Tully's catalog. Since each of the categories of objects with nuclear emission in our subsample cover a wide range in morhological type and include S0/elliptical galaxies which have little dust extinction, and since the completeness function in Sandage et al. (1979) was evaluated for early–type objects, we decided to evaluate the luminosity functions for the absolute magnitudes corrected for galactic and intrinsic extinction ($M^o_{B_T}$) instead of the usual M_{B_T}. To derive them we used the values of the galactic (A_g) and intrinsic (A_i) extinctions listed in the RC3.

Due to the fact that our subsample does not contain many objects per absolute magnitude bin for each of the activity categories, we have to derive the luminosity functions for each of them *including* all the objects in the category. As it is widely known, luminosity functions of clusters differ from those of field galaxies at the faint end (Binggelli et al. 1988), so our luminosity function parameters might be somewhat affected by the Virgo cluster objects. Table 2 lists the percentage of objects in the Virgo cluster for each of the activity categories in our subsample. As can be clearly seen Virgo cluster objects are a small proportion of each category and also within

Table 2. Relative proportion of Virgo cluster objects.

Type	N_V*	N_{tot}*	Percentage%*
HII	17	198	9±2
LINER	11	88	12±4
Seyfert	8	45	18±7
Transition	11	65	17±5

* N_V is the number of objects that belong to the Virgo cluster and N_{tot} the total number in each category. The 1σ errors quoted were derived from pure counting statistics assuming a Poisson distribution.

the errors (pure counting errors from Poisson statistics) all the categories have a similar proportion of objects in that cluster, which guarantees the consistency of our luminosity function estimates.

3. Evaluation of the Luminosity Functions

Following Binggelli et al. (1988), we will use the convention that the number of galaxies lying in a volume dV at (x,y,z) with absolute magnitudes in the range M–M+dM can be represented as:

$$N(M,x,y,z) = \varphi(M)D(x,y,z)dMdV \quad (1)$$

where

$$\int_{-\infty}^{\infty} \varphi(M)dM = 1 \quad (2)$$

$\varphi(M)$ gives the fraction of galaxies per unit magnitude having absolute magnitudes in the interval (M, M+dM) hereafter called the *luminosity function*. $D(x,y,z)$ gives the number of galaxies (of all magnitudes) per unit volume at (x,y,z), hereafter called the "*density function*" following Binggelli et al. (1988). As we will show, for the method of evaluation that we will use in this paper, the density function cancels out in the evaluation equations and therefore the luminosity function can be evaluated directly (except for a normalization constant that will not be considered in this paper).

Several different methods of calculating luminosity functions have been proposed in the literature (see the excellent reviews in Binggelli et al. 1988, Efstathiou et al. 1988 and Willmer 1997). Unfortunately, due to the fact that our sample is based on the RSA catalog which covers only the nearby Universe, powerful methods like the V/V_m estimator (Huchra and Sargent 1973) cannot be used due to its inherent assumption of spatial uniformity, which is certainly not valid in the neighbourhood of the Local Supercluster. Of all the possible estimators that are insensitive to the density functions and that do not assume any a priori spatial distribution, we opted to use one which relys on simple functional representations of $\varphi(M)$ as opposed to the multiparametric methods (i.e., $\varphi(M)$ parameterized for fixed or variable absolute magnitude intervals)(see for instance Marzke et al. 1994) for the sake of simplicity (fewer parameters to fit) and easier interpretation. Furthermore, as we will show later, the goodness-of-fit of the functional representation of the luminosity function can be tested.

Since the total number of objects in some of the activity classes and their absolute magnitude bins are small, we decided to test some of the most widely used functional estimators in the literature at low count levels. This allows us to choose the best method to use. We selected the estimator in Kishner et al. (1979) and the maximum likelihood method outlined in Sandage et al. (1979). The functional representation of the luminosity function was selected to be a 3-parameter Schechter function (Schechter 1976) of the form:

$$\varphi(M)dM = 0.4ln(10)\phi_* 10^{0.4(1+\alpha)(M_*-M)} e^{-10^{0.4(M_*-M)}} dM \quad (3)$$

The estimator used by Kishner et al. (1979) is based on the assumption that for a narrow absolute magnitude interval (*M–M+dM*) and within the volume where a magnitude-limited sample is complete, if we take the ratio of the number of galaxies in the interval *dM*, *N(dM)* to the total number of galaxies brighter than M, *N(≤M)* we obtain:

$$\frac{N(dM)}{N(\leq M)} = \frac{10^{0.4(1+\alpha)(M_*-M)} e^{-10^{0.4(M_*-M)}} dM}{\int_{-\infty}^{M} 10^{0.4(1+\alpha)(M_*-M')} e^{-10^{0.4(M_*-M')}} dM'} \quad (4)$$

where as can be clearly seen, the normalization constant of the Schechter function (i.e., ϕ_*) and the density function in equation 1 cancel out. Therefore, a fit to the ratio values on the left side of the above equation using the function on the right side would provide a direct estimate of the *shape* parameters of the luminosity function, while normalizations could be later evaluated forcing the integral luminosity function to be equal to the total number of objects in each of the subsamples we use. We implemented a fitting routine using a χ^2 minimization with a parametrized optimization algorithm (Marquart's method) and weighting the ratio values with errors estimated from pure counting statistics. To test this estimator for small number of objects, we generated sets of random data points assuming a uniform spatial distribution, a Schechter luminosity function with the typical field galaxy parameters α=-1 and M_*=-21 and an apparent magnitude limit for our sample of 12.5 mag. Simulations were stopped whenever the number of objects for each of the subsamples that we have was reached. Fits were carried out for a range of constant absolute magnitude binnings from 0.2 to 0.6 mag in steps of 0.1 mag.

The main result of these tests was that this method is not adequate for the treatment of the kind of data that we will be dealing with in this paper for the following reasons: (i) there seems to be a very strong dependence of the final fit parameters on the magnitude binning used, in the sense that larger binnings tend to produce poorer fits (the differences are much larger than any conservative error estimate) possibly due to the small number of fit points and their intrinsic noise, and (ii) the information for fainter magnitudes is not used when estimating the ratio values, which makes the faint-end fit quite uncertain. Further problems relating this method have also been outlined by Efstathiou et al. (1988) and Willmer (1997). For the above reasons and after extensive testing, we decided *not* to use this method in this paper.

The maximum-likelihood method proposed in Sandage et al. (1979) is minimally biased by nonuniform density fields, easily accomodates known variations in the magnitude limit of catalogues, and accounts for random errors in the apparent magnitudes. Briefly, the basics of this estimator are that whenever the luminosity of a galaxy can be considered independent of position, the probability that a galaxy of absolute magnitude M_i and redshift z_i is included in a sample with apparent magnitude limit m_{lim} is given by:

$$p_i \propto \frac{\varphi(M_i)}{\int_{-\infty}^{M_{min}(z_i)} \varphi(M')dM'} \tag{5}$$

where $M_{min}(z_i)$ is the minimum absolute magnitude that could be detected at redshift z_i in a catalogue with limiting magnitude m_{lim}, i.e.:

$$M_{min}(z_i) = m_{lim} - 5log(cz_i) + 5log(H_o) - 25 \tag{6}$$

The likelihood that a sample of N galaxies is drawn from the parent distribution $\varphi(M)$ is therefore the product of these probabilities:

$$\Lambda = \prod_{i=1}^{N} p_i \tag{7}$$

The best estimate of the luminosity function parameters is obtained by maximizing the likelihood function or its logarithm (i.e., $\log(\Lambda)$) with respect to the free parameters (α and M_* in our case). As in the previous estimator, the normalization constant of the Schechter function and the density function cancel out in the ratio involved in the probability estimation. The maximization equations derived from partial derivatives of the logarithm of the likelihood with respect to the Schechter parameters are, for α:

$$\sum_{i=1}^{N} M_i = \sum_{i=1}^{N} \frac{I_2}{I_1} \tag{8}$$

and for M_*:

$$\sum_{i=1}^{N} 10^{0.4(M_*-M_i)} = \sum_{i=1}^{N} \frac{I_3}{I_1} \tag{9}$$

respectively, where:

$$I_1 = \int_{-\infty}^{M_{min}(z_i)} 10^{0.4(1+\alpha)(M_*-M')} e^{-10^{0.4(M_*-M')}} \tag{10}$$

$$I_2 = \int_{-\infty}^{M_{min}(z_i)} M' 10^{0.4(1+\alpha)(M_*-M')} e^{-10^{0.4(M_*-M')}} \tag{11}$$

$$I_3 = \int_{-\infty}^{M_{min}(z_i)} 10^{0.4(2+\alpha)(M_*-M')} e^{-10^{0.4(M_*-M')}} \tag{12}$$

A routine for the optimization of this set of two nonlinear equations using a generalization of the Newton-Raphson method to multidimensional parameter spaces (Press et al. 1986) was implemented. The same data files used in the test of the other estimator mentioned above were used and excellent agreement with the original parameters input in the simulated data was found, with only a very weak dependence on the number of objects used in the samples (always well within the 1σ errors estimated below), in agreement with Willmer's (1997) conclusions. We therefore opted for the use of this estimator in this paper.

Error estimates were derived using both the specific formulae for the maximum likelihood method in Efstathiou et al. (1988) (used in the tables below), which give errorbars for each of the two fit parameters separately as well as the 1σ ellipse errors (for the plots below). These come from solving the equation $ln(\Lambda) = ln(\Lambda_{max}) - ln(0.3174)$, where Λ_{max} is the value of the likelihood, when the fit parameters are used in its equation, and the term $ln(0.3174)$ comes from the requirement that we are sampling exactly the 1σ contour of the Λ distribution, that is $\Lambda/\Lambda_{max} = 1 - 0.6826$.

We further can test whether the functional form of the luminosity function that we selected (Schechter's function) adequately represents the data points from each of the subsamples using the method outlined in Yahil et al. (1991). The method is based on the fact that the observed absolute magnitude distribution of a magnitude-limited catalogue will be a representation of the underlying luminosity function mediated by the effect of the sample being distributed in space, which will decrease the number of objects at the faint end due to the flux detection limit. The fact that very bright galaxies are scarce produces an additional drop of the distribution in the bright end. If an estimate of the shape of the luminosity function can be obtained, it is possible to infer an absolute magnitude distribution from the redshift data distribution and magnitude limit. That can be compared

Table 3. Fitted luminosity function parameters.

Subsample	α	M_*
ALL	-0.8±0.1	-20.5±0.1
HII	-0.8±0.1	-20.3±0.1
LINER	-0.5±0.2	-20.5±0.3
TRANSITION	-0.2±0.2	-20.3±0.4
SEYFERT	-0.7±0.2	-21.0±0.3

with the observed absolute magnitude distribution with a simple χ^2 test to deduce whether the assumed functional dependence of the luminosity function is a good representation of the data. To test the goodness of the fits that we present in the next section, we evaluated the following summation for absolute magnitude bins of 0.5 mag covering the whole range of absolute magnitudes in Ho's sample:

$$P(M_i) = \sum_{i=1}^{N} \frac{\varphi(M_j)}{\int_{-\infty}^{M_{lim}(z_i)} \varphi(M')dM'} \quad (13)$$

where the summation is over all the objects in each subsample, M_j represents the central magnitude in each of the bins, M_{lim} is the same as in equation 6, and the luminosity function uses the fitted free Schechter parameters in each case. $P(M_i)$ is proportional to the expected number of objects in each magnitude bin for a given redshift distribution, and its summation over all the magnitude bins gives the total number of objects in the subsample. This can be used to conveniently scale the probability to compare with the observed distribution (binned in magnitude in the same way) using the χ^2 test. χ^2 was only evaluated for those bins that had more than 2 counts and a pure Poisson noise was assumed for each observational bin.

4. Results

The Schechter parameters fitted using the maximum-likelihood method described in the previous section and the 1σ errorbars derived from the formulae in Efstathiou et al. (1988) are listed for each subsample of nuclear activity and for the sample as a whole (i.e., noted as ALL) in Table 3.

As expected, the errorbars are larger the smaller the number of objects in each subsample. Since, as can be seen in Table 1, the number of objects in the LINER and Seyfert subsamples is already fairly small, we did not try to subdivide the Seyferts into types 1 and 2 when evaluating the luminosity functions. In the case of Seyfert galaxies, the so-called "unification models" (Antonucci 1993) propose that both types of objects are intrinsically similar, so a single luminosity function could apply to the whole Seyfert population. Things are less clear for LINERs, which seem to be mostly type 2s and may comprise a variety of different classes of low-luminosity objects (Filippenko 1996). Although it is not possible with our present sample, it would be interesting to evaluate the luminosity function for LINERs when their nature becomes more clear and their possible subdivisions are surveyed with techniques similar to those used by Ho and collaborators. It also should be noted that the values cited for the M_* and α parameters in the case of the ALL sample do not need to be the canonical values for field galaxies cited in the literature (i.e., -21, -1, respectively, Binggelli et al. 1988) both because we are using a Hubble constant of 75 instead of the value of 50, and we have been using absolute magnitudes corrected for galactic and internal extinction instead of the standard B_T values. This will alter somewhat the shape of the luminosity function since the intrinsic dust extinction corrections vary along the Hubble sequence. We have not included the normalization constant ϕ_* values in the table because we are basically interested in the intrinsic shapes of the luminosity functions and this constant will be only a scaling factor proportional to the actual number of objects in each subsample.

Since the errors in the determination of the Schechter parameters are correlated, a better way of displaying the fits and their errors is the determination of the error ellipses via the method outlined in the previous section and plotting the results in two dimensions. This is shown if Figure 1 for the 4 subclasses of activity and for the whole sample. As can be clearly seen, within the errors, the subclasses LINER, Transition and Seyfert seem to have similar luminosity functions. Furthermore, they are clearly separated from the HII subclass. From the plot, it also seems that the designation "Transition object" is not adequate in terms of luminosity functions, since although their spectrum may be a mixture of LINER and HII features, they occur in objects similar to those of the LINER class, and should be therefore considered as LINERs with HII emission (we will return to this point in the Discussion section). The general displacement to fainter M_* of the HII subclass with respect to the other groups, suggests that these objects tend to be located in later Hubble types, as can be clearly seen in Ho et al. (1997b).

As mentioned in the previous section, we have assumed ad hoc a definite functional dependence for the luminosity function (i.e., a Schechter function). Although that may be a good approximation to the general field galaxy population, it may not represent the data in the subsamples that we have that are more restricted in Hubble type. To test the goodness of the fits and the adequacy of our assumption, we have used the χ^2 test described in the previous section for each subsample. The results of

Table 4. χ^2 test on the assumed luminosity function.

Subsample	χ^2	df*
ALL	6.78	10
HII	15.94	10
LINER	2.98	5
TRANSITION	2.53	5
SEYFERT	5.88	6

* Number of degrees of freedom calculated as the number of 0.5 mag absolute magnitude bins with more than two counts in the range of absolute magnitudes covered by out whole sample minus the number of free parameters in the fitted Schechter luminosity function.

the tests are shown in Table 4.

Except for the HII subsample, all the values of χ^2 indicate good fits. To investigate this discrepancy, we plotted the absolute magnitude distribution of the HII subclass and compared it with that of the other groups. As can be clearly seen in Fig. 2, HII show a secondary peak at absolute magnitudes around -18 or less which does not appear in any of the others. When this second peak was investigated, we found that it is primarily due to a number of dwarf and Im galaxies. This seems to indicate that the HII luminosity function is actually bimodal, with a contribution from the dwarf galaxies superposed on a more general Schechter-like function. We checked this by refitting the luminosity function for the HII subsample without any of the dwarf or Im galaxies. In that case we obtained a quite better fit (i.e., χ^2=12 for df=9) at α=-0.6 and M_*=-20.2 with errorbars and error ellipses similar to those in table 3. This point is still separated from the rest of the subclasses even considering the 1σ ellipses, which strengthens our previous result that HII objects are a separate class. Furthermore, this result seems to suggest that for dwarf/late type galaxies, the dominant type of nuclear activity is star formation.

We have also tried to compare our results for Ho's sample with other catalogues of active objects in the literature. Unfortunately, it turns out that a comparison for the HII class is quite difficult due to the fact that most catalogues are biased to the high FIR luminosity objects which are mostly very distorted galaxies for which B_T^o estimates are very difficult. We expect that our results represent the low to mid FIR luminosity population of starbursts. For Seyferts and LINERs several studies have been published in the literature, but most of them suffer from different kinds of biases. The only survey that attempts to overcome most of them is the CfA Redshift Survey, which is a purely spectroscopic with a limiting apparent Zwicky magnitude of 14.5 mag, and contains 48 Seyferts and 31 LINERs (Huchra and Burg 1992). A completeness study of the active galaxies in this catalog, though, shows that LINERs are heavily undersampled at faint magnitudes (Huchra and Burg 1992), and therefore we can only use the Seyfert subsample. As for our sample, we evaluate the total luminosity function of both types of Seyferts. Since a comparison of the B_T magnitudes in the RC3 with those m_b magnitudes in the B(0)-ZW system listed in Huchra and Burg (1992) show an offset of 0.25 mag, we have assumed that in the B_T system, the Seyfert sample is complete to 14.25 mag and used our software to calculate the luminosity function as above. As can be seen in Fig. 1, although the CfA sample is compatible within the error ellipse with the values we deduce for our sample, the mean values are fairly offset from them. This can be easily understood if we assume that the CfA sample, since no adequate continuum substraction technique has been used, is only sampling intrinsically bright (in nuclear line emission) objects that lie in bright galaxies (an inspection of the list shows that there are no detections for objects fainter than M_T^0=-17, while there are several in our sample). Therefore, we conclude that, although the CfA sample is a good representation of the bright end of the Seyfert luminosity function, it does not cover the faint-end, both in line emission and galaxy hosts, which are better covered by Ho's work.

Huchra and Burg (1992) point out the possibility that when the number of objects on either side of M_* is small, a large covariance between α and M_* may be present. This covariance would in our case affect the conclusions on the low luminosity end of the luminosity function. To test that the main conclusions of the fits are right, we have also computed the luminosity function for each subsample by simply binning by absolute magnitude, counting the number of objects per bin, and dividing it by the mean search volume at the center of the absolute magnitude bin (Huchra and Burg 1992). As already mentioned before, this kind of luminosity function estimate is very dependent on the local inhomogeneities of the galaxy density (particularly large within the Local Supercluster), and therefore will only be used here to compare the properties of the faint-end of the luminosity functions. Fig.3 shows the calculated luminosity functions for the HII, LINER+Transition and Seyfert subsamples (as we discuss below, LINERs and Transition objects form a single class from the point of view of the luminosity function). The humps seen in each of them in the range -18 to -19 mag is due to the increase of apparent density due to the Virgo cluster. Regarding the faint-end region, it can be clearly seen that the HII class has a different behaviour than the LINERs and Seyferts (the latter has a small number of objects below -18), supporting the results of our fits. While the luminosity functions of LINERs and possibly Seyferts tends to flatten at lower luminosities, the one for the HII galaxies increases. The

Fig. 1. Maximum-likelihood fitted Schechter parameters α and M_* for the whole (ALL) and HII, LINER, Transition objects and Seyfert subsamples. 1σ error ellipses for each of the fits is also shown. The position of the fit for the HII subsample without Im and dE galaxies is indicated with an arrow starting in the fit position to the whole subsample. The position of the fit to the Seyfert sample in Huchra and Burg (1992) is also shown as "CfA Seyferts" (see text).

faster flattening of the Seyfert luminosity function also explains the difference in the M_* values with the other subsamples. We therefore conclude that our Schechter fits reflect true tendencies of the subsamples and proceed to discuss the main implications of these results.

5. Discussion

We proceed to discuss several different issues that originate from this work:

5.1. What are the Transition Objects?

Transition objects were first defined by Ho and Filippenko (1993), and include those objects that appear to have nuclear emission line spectra with line ratios that fall in intermediate zones between the LINER and the HII class. As we showed above, the luminosity functions for LINERs and Transition objects seem to be quite similar, which suggests that both subclasses of objects occur in fairly similar hosts (early-type galaxies). However, a careful inspection of both subsamples shows that there are some differences. One of them is the fact that there seems to be a higher proportion of elliptical galaxies in LINERs (23%) than in Transition objects (8%). Another important difference is that there seems to be a higher proportion of high inclination spirals in the Transition subclass (for distances up to 40 Mpc, 86% of the Transition objects have inclinations higher than 40 degrees, compared with 60% of the LINERs). Taking into account that ellipticals have lower current star formation rates than spirals, the fact that Transition objects tend to lie in similar spiral types as LINERs but have higher disk inclinations, and the fact that Transition and LINERs, as shown above, clearly differ from the HII subclass, it seems natural to deduce that Transition objects are just LINERs that, due to the high inclination of the disk and the fixed spectrograph aperture used in Ho's survey, are contaminated by HII regions from the disk or circumnuclear regions. Transition objects should not be considered a sepatare class from LINERs. For the few ellipticals in the transition subclass, there has been no study of their current star formation rate, but it is quite possible that they are systems similar to the nearby S0 galaxy NGC404, where a LINER nucleus is surrounded by current star formation (Cepa et al. 1997). Due to the system being observed almost face-on and being a nearby

Fig. 2. Comparison of the absolute magnitude distribution of the LINER+Transition Object subsamples (a) and the HII subsample (b). The LINER and Transition Object subsamples were merged folliwing the discusion in the text that they are the same kind of objects.

object, an aperture of only a few arcsec would produce a spectrum dominated by the nuclear LINER, but if the system was viewed at higher inclinations, HII region contamination would change its classification to Transition.

5.2. LINERs vs. Seyferts

This time, it is not at all clear what powers LINERs. Although there are some cases which have broad Balmer lines, clearly placing them in the AGN group, there is a quite larger proportion of type 2 objects in the LINER class than in Seyferts (Ho et al. 1997b). Therefore, we are left with two possible scenarios. One is that, following the so-called "unified models" of AGNs, LINERs are the low luminosity end of AGNs and that there is a tendency for low luminosity AGNs to have dusty/obscuring torii with larger covering factors or the nuclear source if "off" for long periods of time (Maoz et al. 1995). The other is that, LINERs are a mixture of objects of quite different origins, some being the low-luminosity extrapolation of the AGN phenomenon and others (which might actually be the majority) produced by other mechanisms like shocks, cooling flows or simply star formation (Filippenko 1996).

In recent years mounting observational evidence has pointed towards a completely new picture of the nuclei of galaxies, in which supermassive BH at the centres of the hosts have are widespread (Kormendy 1995). Furthermore, these observational results also suggest that the masses of these nuclear BHs are somehow related to the masses of the bulges, which would indicate that early type galaxies tend to have more massive BH. In view of this, the former scenario cited above (i.e., most LINERs are AGNs) would imply, since we deduce that the luminosity functions of Seyferts and LINERs are very similar (they lie in similar Hubble type hosts, mostly early-type objects), that LINERs contain poorly fueled central BHs. This could be compatible with the higher proportion of type 2 LINERs if somehow gas moving radially inwards toward the center due to some large scale dynamical mechanisms might be piling up at intermediate scales (due to resonances) and not proceeding further in, or with the possibility that the nucleus flares-up only sporadically due to some accretion of a star near the central BH (Maoz et al. 1995). The only problem that the authors can see with this view is that a fair number of objects (specially ellipticals) show *extended* LINER emission (Filippenko 1996). It is our feeling that this certainly points to the possibility that at least two kinds of LINERs exist: those objects powered by nuclear sources (that may be more abundant in spirals) and the other those powered by extended sources like cooling flows or AGB stars. Fast shocks in strong magnetic field environments have also been suggested as other possible sources of nuclear ionization (Dopita and Sutherland 1996), together with several stellar ionization mechanisms (O-type stars, warmers, etc.). Radio jet induced shocks have proved to be quite successful in explaining the NLR emission in some Seyfert galaxies and recent work suggests that they can actually explain most of the optical spectra (the UV region has still not been properly explored and seems to be the region that can discern between shock or photoionization) (Wilson and Raymond 1999). According to these models, the spectral differences between Seyferts and LINERs would only be due to the fact that, although they experience the same kind of fast shocks, LINERs would have less gas in the path of the jets. If that is true, high-sensitivity radio surveys like those in Seyferts should have revealed the presence of jets, but till present only compact sources seem to have been detected (Condon 1996). We also point out that shocks would ultimately originate from AGN related activity and that therefore LINERs should still be the low-luminosity end of the AGN sequence. All stellar ionization-related models postulated to date seem to have problems explaining LINER properties as a whole (Filippenko 1996), but can still explain some of the objects, so they may also be a part of the LINER population.

In summary, our result that the luminosity functions of LINERs and Seyferts are similar suggests that Seyfert and LINER activity seems to occur in similar Hubble type hosts as a whole. However, the larger proportion LINERs which are elliptical galaxies and type 2 objects, together with the presence of extended LINERs, suggest

Fig. 3. Differential luminosity functions of HII, LINER+Transition and Seyfert galaxies derived from pure volume-averaged magnitude-binned counting (see text). Errorbars were calculated from the source numbers in each bin assuming Poisson statistics.

that LINERs are a mixture of different kinds of objects. Although it is still quite possible that a large number of LINERs are micro-AGNs, there is certainly a proportion of them that originate from other mechanisms. At present, we cannot give a better estimate of the real low luminosity end of the AGN population in the nearby Universe.

5.3. Low luminosity Seyferts

A very important question that Ho's sample allows us to address is the relative percentage of Seyfert galaxies in low luminosity hosts. This has been addressed in the past, but due to sample biases, the only conclussion that could be reached was that Seyfert galaxies tend to lie in luminous hosts. If they really were *only* concentrated in such hosts, we would expect that their luminosity function would have a very sharp decrease at low luminosities (i.e., an α parameter close to zero or even positive). However, we find that although there is a clear decrease of the number of Seyferts at low luminosities, their decrease is just somewhat steeper than the HII objects. In fact, an inspection of our sample reveals that 17% of the Seyferts at distances below 12 Mpc have absolute magnitudes fainter than -18 mag (and one of the objects, NGC185, is as low as -15). Even taking into account Malmquist bias imposed by the RSA catalog magnitude limit, this implies that a substantial number of low luminosity hosts *do* actually contain Seyfert nuclei. We note, however, that this is not in contradiction with previous works in the sense that those works could only detect brighter objects due to the observational and data reduction techniques that were used. Since our Seyfert subsample does not contain a large number of objects, it is still difficult at present to assess the relative proportion of low-luminosity-host Seyferts, but even coping for the errors in our fit, this proportion may be actually larger than the number of objects at the high-luminosity end.

Since Ho's survey is quite deep and also since the bulge stellar decontamination is quite good, very weak Seyfert nuclei have been detected. The question remains whether there is any trend of the nuclear line luminosities with the properties of the hosts. Unfortunately, due to the combined effect of the Malmquist bias and the fact that the nuclear spectra were taken with a fixed aperture, added to the fact that the Seyfert subsample does not contain many objects makes it very difficult to infer any trends. As can be seen if Figure 4a, the average Hα luminosities evaluated in 1 mag. bins (for each bin only the objects

Fig. 4. Mean nuclear Hα luminosities as a function of the absolute magnitudes of the hosts (a) and Hα luminosities vs. distance for hosts with absolute magnitudes in the range -21 to -20 mag (b) for the Seyfert subsample. The errorbars in (a) are the 1σ rms values of the distribution for each magnitude bin.

up to the maximum distance that can be reached with a 12.5 apparent magnitude limit were used) seem to decrease with host absolute magnitude, but this decrease can be easily explained as a decrease in the fraction of the NLR (Narrow Line Region) that is observed with the fixed aperture in Ho's survey, as shown in Fig. 4b for the absolute magnitude range -22 to -21. The clear increase in Hα luminosity (but similar scatter) with distance for a magnitude range that is not affected by the Malmquist bias up to 70 Mpc can only be explained by an aperture effect. Furthermore, as can be seen in that Figure, the variation range is similar to that in Fig. 4a. A similar spectroscopic survey of deeper catalogues is needed to solve this dilemma.

Another question that can be addressed here is whether there is any difference between the hosts of Seyfert types 1 and 2. This point is specially relevant since some authors have suggested the possibility that going to weaker nuclear line fluxes might change the whole picture of the "unified models" drastically. Due to the small number of objects that would result if we further subdivide the Seyfert subsample into types (which would result in meaningless luminosity function estimates), the only test that can be carried out with the present dataset is on their average properties. Assuming that any object that has not been specifically classified as type 2 in Ho's listings is a Seyfert type 1, we performed a Kolmogorov-Smirnov test on the absolute magnitudes (at this luminosity levels, the nuclear blue continuum is not expected to contribute much to the TOTAL blue magnitude of type 1s). With a very high significance (0.6) we find that both types of Seyferts seem to have been extracted from the same parent population of objects (there is no systematic difference in the detection rates of any of the two types of Seyferts with distance, but there is some clear tendency to low detection levels at high host disk inclinations). Although this result needs to be taken with caution since we are dealing with small samples, it suggests that faint Seyfert galaxies are not much different from objects with higher nuclear line luminosities.

We would like to thank Drs. Nario Kuno, Kazushi Sakamoto, Kotaro Kohno, and Kazuo Sorai for their illuminating discussions on some of the critical parts of this paper. We also thank the referee John Huchra for his comments that greatly helped to improve the scientific and grammatical contents of this paper.

References

Antonucci R. 1993, ARA&A 31, 473
Baldwin J.A., Phillips M.M., Terlevich R. 1981, PASP 93, 5
Binggelli B., Sandage A., Tammann G.A. 1988, ARA&A 26, 509
Bregman J.N. 1990, A&AR 2, 125
Cepa J., Vila-Vilaro B., Nakai N., Kohno K., Kawabe R. 1997, IAU Symp. 187, 130
Choi Y., Yang J., Yi I. 1999, ApJL 518, L77
Condon J.J. 1996, ASP Conf. Ser. 103, 132
de Vaucouleurs G., de Vaucouleurs A., Corwin H.G., Buta R.J., Paturel G., Fouqué P. 1991, Third Reference Catalogue of Bright Galaxies, Springer Verlag
Dopita M.A., Sutherland R.S. 1996, ApJS 102, 161
Efstathiou G., Ellis R.S., Peterson B.A. 1988, MNRAS 232, 431
Filippenko A.V. 1996, ASP Conf. Ser. 103, 17
Heckman T.M., Gonzalez-Delgado R., Leitherer C., Meurer G.R., Krolik J., Wilson A.S., Koraktar A., Kinney A. 1997, ApJ 482, 114
Ho L.C., Filippenko A.V. 1993, ApJ 417, 63
Ho L.C., Filippenko A.V., Sargent W.L.W. 1997, ApJS 112, 315
Ho L.C., Filippenko A.V., Sargent W.L.W. 1997b, ApJ 487, 568
Huchra J., Burg R. 1992, ApJ 393, 90
Huchra J., Sargent W.L.W. 1973, ApJ 186, 433
Kim D.W., Elvis M. 1999, ApJ 516, 9
Kim D.C., Sanders D.B. 1998, ApJS 119, 41
Kishner R.P., Oemler A., Schechter P.L. 1979, AJ 84, 951
Koehler T., Groote D., Reimers D., Wisotzki L. 1997, A&A 325, 502
Kormendy J. 1995, ARA&A 33, 581
Maoz D., Filippenko A.V., Ho L.C., Rix H.W., Bahcall J.N., Schneider D.P., Macchetto F.D. 1995, ApJ 440, 91
Marzke R.O., Huchra J.P., Geller M.J. 1994, ApJ 428, 43
Moorwood A.F.M. 1996, Space Sci. Rev. 77, 303

Press W.H., Flannery B.P., Teukolsky S.A., Vetterling W.T. 1986, Numerical Recipes (Cambridge Univ. Press, Cambridge)
Rees M.J. 1984, ARA&A 22, 471
Sandage A., Tammann G.A., Yahil A. 1979, ApJ 232, 352
Sandage A., Tammann G.A. 1981, A Revised Shapley-Ames Catalog of bright Galaxies (Carnegie Institution of Washington, Washington D.C.)
Schechter P.L. 1976, ApJ 203, 297
Tully R.B. 1988, Nearby Galaxies Catalog (Cambridge Univ. Press, Cambridge)
Willmer, C.N.A. 1997, AJ 114, 898
Wilson A.S., Raymond J.C. 1999, ApJL 513, L115
Yahil A., Strauss M.A., Davis M., Huchra J.P. 1991, ApJ 372, 380

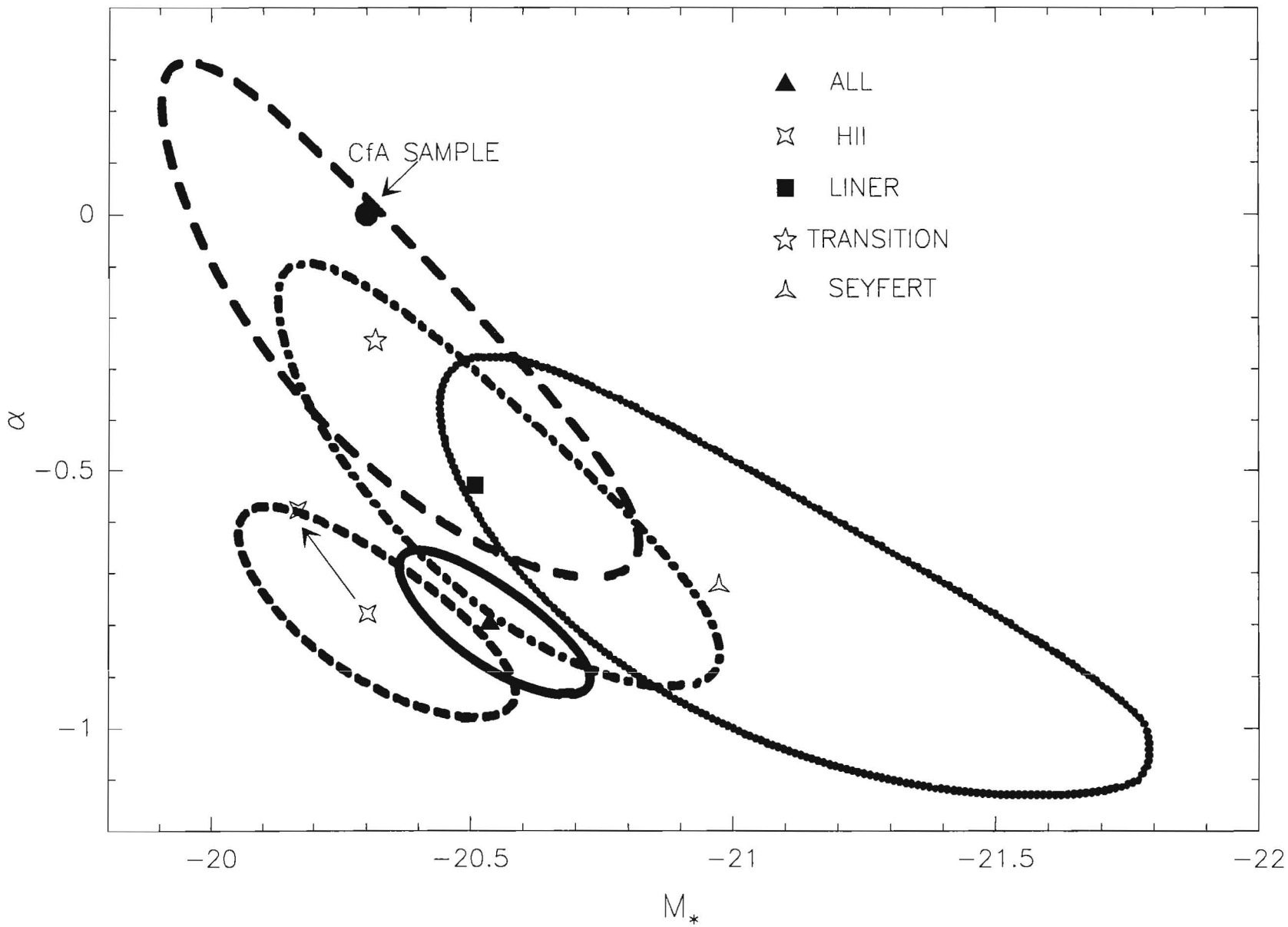
ALL
HII
LINER
TRANSITION
SEYFERT
CfA SAMPLE
0
−0.5
−1
α
−20
−20.5
−21
−21.5
−22
M*

Fig. 1

Fig. 2

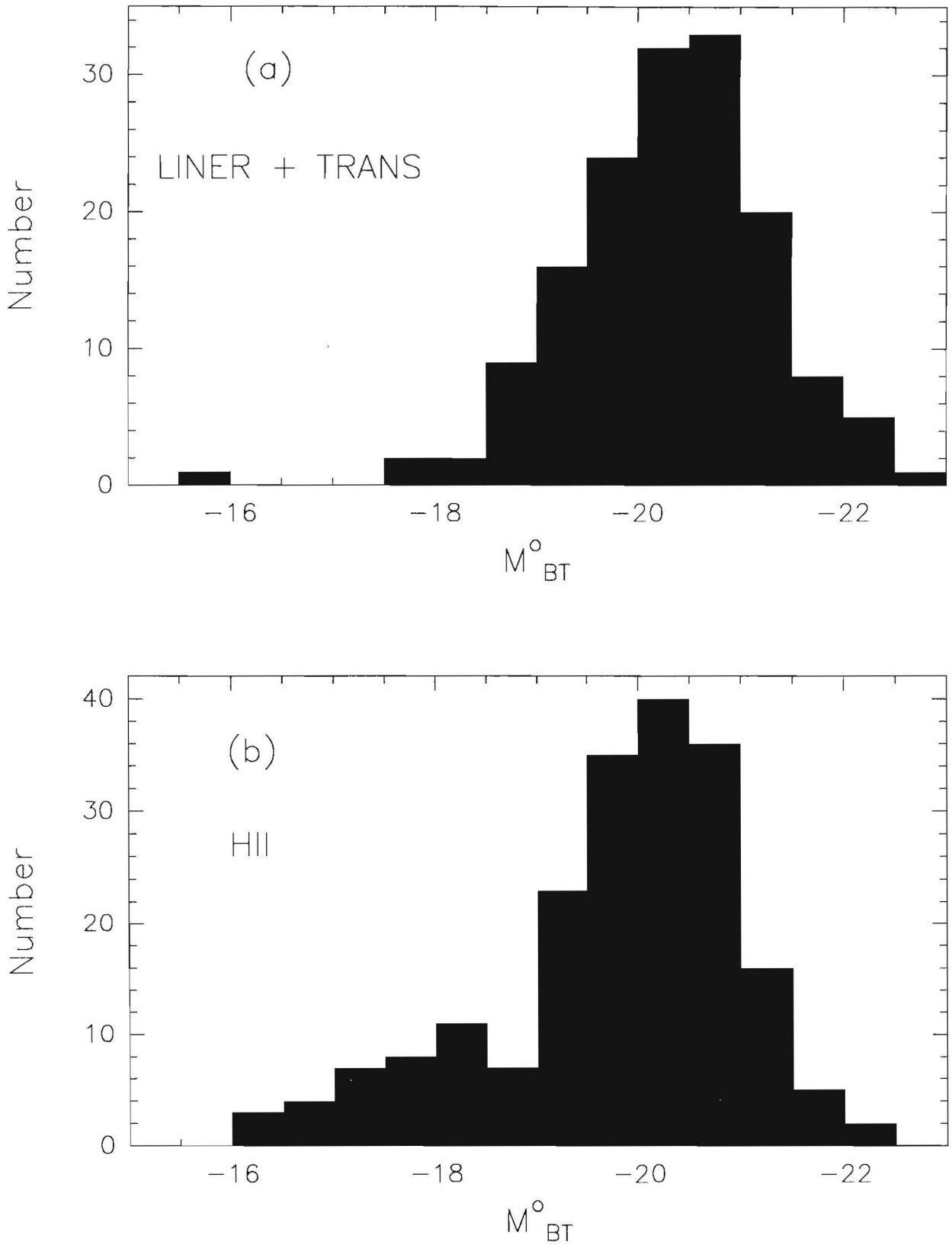
(a)
LINER + TRANS
Number
0
10
20
30
−16
−18
−20
−22
M°BT
(b)
HII
Number
0
10
20
30
40
−16
−18
−20
−22
M°BT

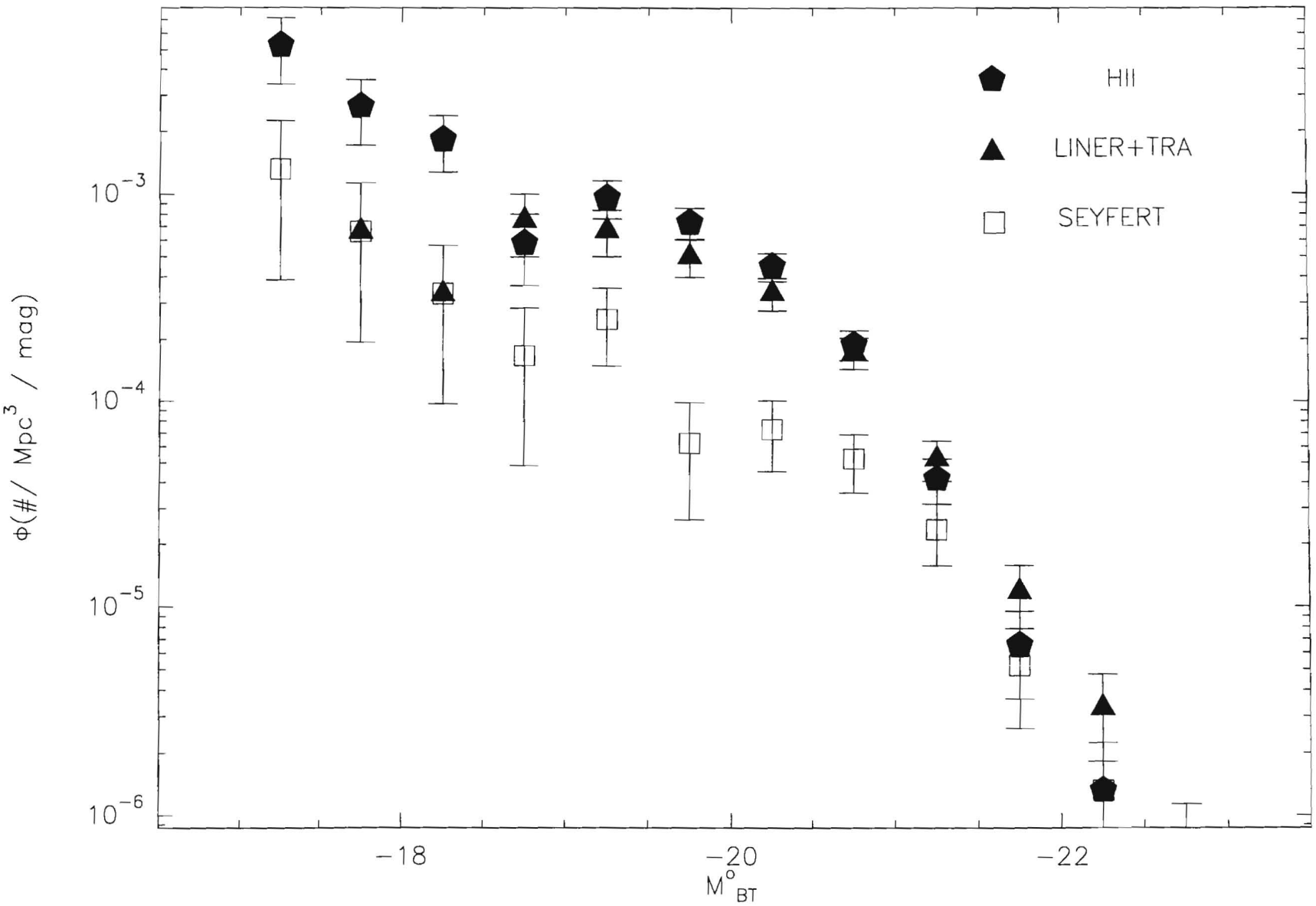
HII
LINER+TRA
SEYFERT
10^{-3}
10^{-4}
10^{-5}
10^{-6}
$\Phi(\#/\ Mpc^3\ /\ mag)$
−18
−20
−22
M^o_{BT}

Fig. 3

Fig. 4

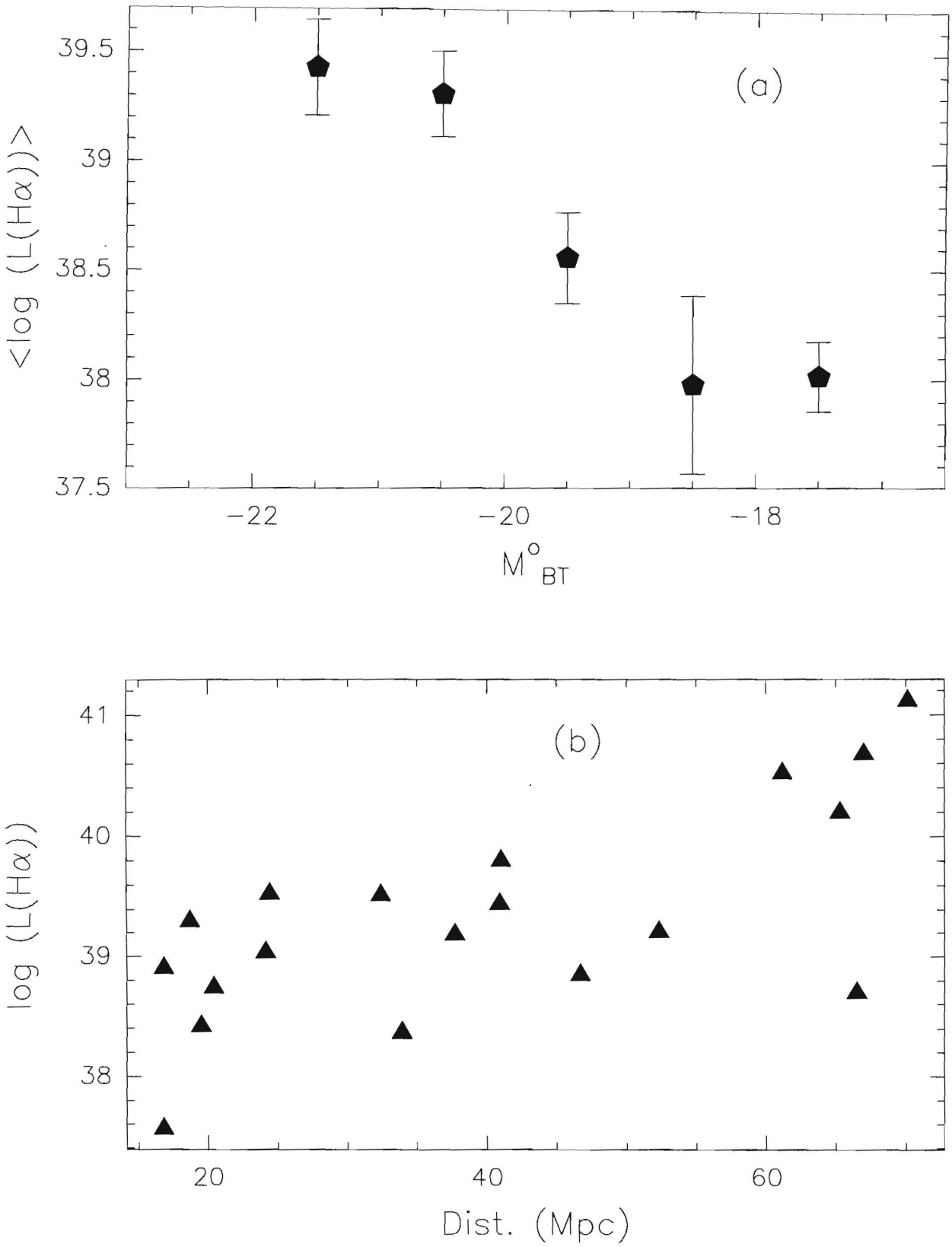
(a)
39.5
39
38.5
38
37.5
<log (L(Hα))>
−22
−20
−18
M°BT
(b)
41
40
39
38
log (L(Hα))
20
40
60
Dist. (Mpc)